Network bypasses sustain complexity

Ernesto Estrada[a,1], Jesús Gómez-Gardeñes[b,c], and Lucas Lacasa[a]

Real-world networks are neither regular nor random, a fact elegantly explained by mechanisms such as the Watts–Strogatz or the Barabási-Albert models, among others. Both mechanisms naturally create shortcuts and hubs, which while enhancing the network's connectivity, also might yield several undesired navigational effects: They tend to be overused during geodesic navigational processes—making the networks fragile—and provide suboptimal routes for diffusive-like navigation. Why, then, networks with complex topologies are ubiquitous? Here, we unveil that these models also entropically generate network bypasses: alternative routes to shortest paths which are topologically longer but easier to navigate. We develop a mathematical theory that elucidates the emergence and consolidation of network bypasses and measure their navigability gain. We apply our theory to a wide range of real-world networks and find that they sustain complexity by different amounts of network bypasses. At the top of this complexity ranking we found the human brain, which points out the importance of these results to understand the plasticity of complex systems.

complex networks | geometric embedding | communicability paths

The advent of Network Science (1, 2) was marked by the urgent need to decipher simple and local mechanistic models underlying the self-organized formation and growth of natural and artificial real-world networks, models able to parsimoniously account for large-scale structural patterns systematically deviating from stylized ones such as purely ordered lattices or purely random graphs. Two such celebrated models, aiming to explain the ubiquitous real-world patterns of "small-worldness" (SW) and "scale-freeness," were proposed in seminal contributions by Watts and Strogatz (3) and Barabási and Albert (BA) (4), respectively. The resulting network topologies of SW and BA networks— poised between order and disorder at the statistical level—were coined as "complex." Here, we give special attention to these as they are paradigmatic mechanisms that create complexity through heterogenization although we acknowledge that other patterns (2)— e.g., communities, assortative, and disassortative mixing, triadic closure, etc.—are also relevant in this context.

Indeed, what is complex in a complex network? Conceptually, system complexification (5) may occur via different types of mechanisms including symbiosis, exaptation, or structural deepening, to cite some. The latter concept of structural deepening (6), which we adopt here, focuses on the situation where the efficiency of an existing function in the system is increased as the system complexifies, where a higher efficiency is usually interpreted in terms of performing the same function using less available energy. Accordingly, a network with a structure poised between total order (lattice) and pure disorder (random graph), such as SW and BA networks as well as many networks in the real-world, is compatible with the existence of a structural deepening mechanism which improves the communication efficiency between the nodes in the networks. Identifying a quantitative proxy that characterizes such structural deepening mechanism in networks remains, however, an open problem, and constitutes the first motivation of this work. As a matter of fact, the Watts–Strogatz mechanism does not provide a clear-cut definition of what an SW network is—only a certain range of network's mean path length and clustering coefficient, indicating that neither of these two network properties are quantitative proxies of a potential structural deepening mechanism. Similarly, the extensive zoology of degree distributions existing in empirical networks (7, 8) points to the fact that observing scale-freeness is not in itself enough to indicate the existence or not of a structural deepening mechanism. Other network properties, such as the node-based fractal dimension (NFD), the node-based multifractal analysis (NMFA), the structural distance, or the degree of complexity (9, 10), suffer from similar problems, and, e.g., fail to identify a specific point within the SW region where structural deepening is maximized.

And yet, networks serve the purpose of facilitating the communication between otherwise isolated entities of a complex system. Therefore, if a structural deepening mechanism exists in the evolution of a network, it is likely that it involves an improvement

Significance

We show here that existing mechanisms of network evolution also create structural network bypasses as by-products: alternative routes to shortest paths that enable collateral circulation, making the system naturally resilient against failure of the widespread topological shortcuts or hubs. We develop a mathematical theory that explains the emergence of bypasses and quantify their impact on aspects such as network navigability gain. We finally apply our framework to analyze a large set of real-world networks and rank them according to the amount of network bypasses they show. At the top of this ranking, we find the human brain, what points out the importance of these results, to understand the plasticity of complex systems.

Author affiliations: [a]Institute for Cross-Disciplinary Physics and Complex Systems, Consejo Superior de Investigaciones Científicas-Universitat de les Illes Balears, Palma de Mallorca 07122, Spain; [b]Department of Condensed Matter Physics, University of Zaragoza, Zaragoza E-50009, Spain; and [c]Group of Theoretical and Applied Modeling (GOTHAM lab), Institute for Biocomputation and Physics of Complex Systems (BIFI), University of Zaragoza, Zaragoza E-50018, Spain

[1]To whom correspondence may be addressed. Email: estrada@ifisc.uib-csic.es.

of some communication efficiency. SW and BA-type mechanisms indeed tend to generate networks with enhanced connectivity (9) (a form of structural deepening) which are robust against random failures (10, 11), what in principle could explain the ubiquity of these mechanisms and the resulting macroscopic patterns, even if quantifying such complexity has proven elusive.

However, observe that the SW mechanism reduces mean path length simply by creating path shortcuts, making enhanced connectivity overly dependent—and thus, fragile—on them. Likewise, in BA-like networks, shortest paths often involve hubs, and these networks are known to be extremely fragile against failure of hubs (12) or jamming (13–16), potentially inducing a failure cascade which can severely harm the macroscopic network's function.

Why, then, complex networks are ubiquitously observed? First, note that walkers navigating a network do not necessarily have full information of the network structure, and geodesic navigation is indeed a global optimization problem (17) that, accordingly, "blind" walkers cannot perform. Second, such blind walkers typically undergo diffusion-like navigation, and such parsimonious navigation strategy can lead walkers to "diffuse out" and get lost easily if attempting to follow shortest paths, as these tend to have higher degree nodes*. Accordingly, nongeodesic navigational strategies have been proposed (18–24), usually providing heuristic recipes based on local network information available [such as the degree (18–20) or the matching index (21)]. Solving the apparent dilemma between the prevalence of complex network architectures—underpinned by WS and BA mechanisms among others—with structural deepening related to enhanced communication capacity requires to find parsimonious mechanisms which can mitigate the undesired effects of geodesic navigability, and this is the second motivation of our work.

Our contention in this work is that as a network complexifies, it is capable to mitigate the impact of the undesired geodesic navigability issues by structural deepening mechanisms which favor the consolidation of network bypasses: alternative routes to mere geodesic navigation that i) decrease the tendency of "getting lost" by blind walkers, and ii) if needed can also be used by nonblind walkers to avoid problematic links and nodes, therefore allowing the overall connectivity to be maintained and the network to be robust against failure of shortcuts and hubs.

In what follows we start from first principles and develop a theory to define and detect the emergence of network bypasses in both synthetic and real-world networks and quantify their associated gain and impact in terms of network navigability. Our theory is based on a network geometrization by which initially unweighted edges and paths acquire an effective weight—an effective length, or cost—induced solely by the topology of the surrounding network's structure. Network bypasses then emerge as geodesic paths in the geometrized network, i.e., they are the solutions of a topology-induced minimum-cost path optimization problem (25), and in many cases, we show that they do not coincide with the shortest paths of the original network. We also show that i) the emergence of these network bypasses is an unavoidable (entropic) by-product of the WS and BA mechanisms themselves and that ii) the effect of these bypasses is optimally emphasized when networks fall in a specific point of SW regime and an intermediate edge density in the sparse regime for BA-like networks, thus finding a quantitative proxy for structural deepening. We also certify that iii) network bypasses indeed provide source–destination routes with better navigation

properties for diffusive-like blind walkers than geodesic routes and finally rank and discuss the emergence of network bypasses and their associated navigability gain in a range of real-world networks.

Results

To fix the intuition, let us begin by illustrating two situations in simple graphs that highlight the importance of bypasses in the operation of a network that harbors transportation and propagation of signals and information. To this aim, we initially consider a particle hopping between the nodes of a network created via the WS model (3), and we focus on the propagation of the particle between nodes i and j (Fig. 1A). Starting with rewiring probability $p = 0$, we have a circulant graph $\mathcal{G}$, and the path $P_1 = \{i, j-1, j\}$ of length 2 (highlighted in blue) is a shortest path connecting i and j. Mimicking the action of WS-like mechanism kicking in, the edge $e = (i, i+1)$ of $\mathcal{G}$ is randomly rewired, and subsequently, another edge is also randomly rewired, so that node $j-1$ now receives an edge from a "distant" node. In the resulting graph $\mathcal{G}'$, vertex $i+1$ drops its degree by one, whereas vertex $j-1$ increases its degree. This situation creates a small degree heterogeneity in the graph $\mathcal{G}'$ which did not exist in the circulant graph $\mathcal{G}$: Node $j-1$ now participates in many more shortest paths starting elsewhere and ending at vertex $j-1$. Accordingly, the length-2 path P_1, in practice, might not be the "best" route to connect i and j, even if it is still the shortest path, topologically speaking. For instance, a random walker choosing P_1 has a higher likelihood of "diffusing out" through $j-1$, thus hardly reaching the destination. Likewise, geodesic navigation will make $j-1$ systematically overused, leading to a higher chance of damage or jamming. In turn, the length-3 path $P_2 = \{i, i-1, i+1, j\}$ (highlighted in pink), while being topologically longer than P_1, contains node $i+1$ whose degree is at the same time lower than the average and also avoids $j-1$; hence, it can be seen as a potentially more ballistic route that avoids a potentially problematic $j-1$ and still connects i and j.

A similar situation is depicted in Fig. 1B where node h becomes a hub via a rich-get-richer (i.e., BA-like) mechanism. The shortest path between i and j (highlighted in blue) will again be more prone for the walker to get lost due to the presence
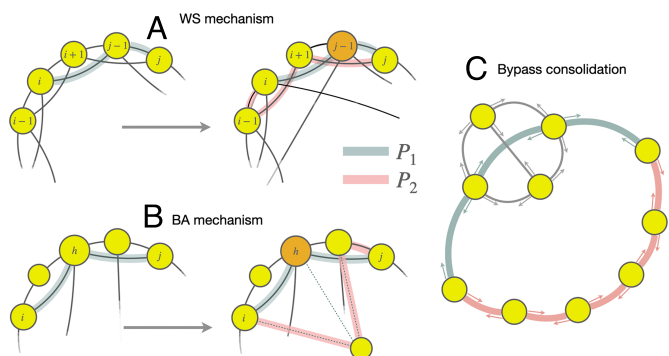

Fig. 1. (*A*) Illustration of the effects of the edge rewiring process in the Watts–Strogatz model on the paths connecting two arbitrary vertices of the resulting graph: the shortest path P_1 (blue) can be bypassed by the path P_2 (pink), topologically longer but with a lower energetic cost. (*B*) A similar phenomenon happens when the node h becomes a hub after a rich-get-richer mechanism. The shortest path P_1 (blue) typically crosses the hub but, with a sufficiently large mean degree, other paths such as P_2 (pink) can bypass the shortest path P_1, allowing alternative routes when hubs reach capacity and become saturated or damaged. (*C*) Navigational dilemma embedded in a network: The blue path P_1 is the shortest path, but it turns out that the pink "braquistochronic" path P_2 is more advantageous as it avoids congestion and is less resistive (see *SI Appendix*, section S5 for an explicit calculation).

---

*A node of degree k potentially connects $k(k-1)/2$ pairs of nodes by shortest paths of length two. Longer SP also uses them to connect other pairs of nodes. Thus, the higher the degree of a node, the higher the number of SP crossing that node.

of a high-degree node, once the BA mechanism enhances such heterogeneity. Now, if the network supports a sufficiently large[†] mean degree—i.e., if the network allows more edges to be formed than a spanning tree—, then other routes can emerge, bypassing the hub (pink path).

The two examples illustrated in Fig. 1 *A* and *B* raise the question of whether a particle would "prefer" to travel from i to j via the shortest—albeit with higher uncertainty to reach the destination—path P_1 or along the slightly longer but more ballistic—smaller uncertainty—alternative path P_2. In Panel (*C*) of the same figure, we illustrate such a conundrum where two alternative routes (a shortest path P_1, in blue, and a topologically longer one P_2, in pink) are highlighted. It is intuitive to think that there is a trade-off: Sometimes, P_1 is to be preferred, sometimes P_2 is a contingently better option. Extending this situation to a network-growth mechanism, this suggests that the creation of shortcuts (SW) and hubs (BA) should be sustained by the emergence of some alternative paths bypassing these, with structural deepening effects that would reach a maximum impact for a specific rewiring probability p (SW) as well as specific hub abundance (BA). In what follows, we introduce a formalism that puts these questions and their general solution in a solid grounding.

The Concept of Resistive Paths. Starting from first principles, the possible trajectories that a hopping particle can perform over a network $\mathcal{G} = (V, E)$ of $|V| = n$ nodes with binary adjacency matrix $\mathbf{A} = \{A_{ij}\}_{i,j=1}^n$ can be enumerated by computing the powers of $\mathbf{A}$. A natural way to penalize longer trajectories connecting the same initial and end nodes is to properly weight them

$$\mathbf{G}(\beta) = e^{\beta \mathbf{A}}; \; G_{ij}(\beta) = \sum_{l=0}^{\infty} \frac{\beta^l (\mathbf{A}^l)_{ij}}{l!} = \left(e^{\beta \mathbf{A}} \right)_{ij}, \quad \textbf{[1]}$$

where β is an empirical parameter. This expression is known as the communicability function of a graph (26, 27). While originally being a purely combinatorial expression that encapsulates the contributions of different walks in a graph, $\mathbf{G}(\beta)$ indeed emerges as a central matrix when analyzing a wide variety of dynamics on graphs (27–31) (see *SI Appendix*, S1.1 for details and S1.2 for a derivation of $\mathbf{G}(\beta)$ as the actual propagator in a specific case with Hamiltonian dynamics). Nowadays communicability is applied across a range of disciplines, from neuroscience (32–39) or cancer research (40) to ecology (41) or economics (42), to cite a few.

While this operator naturally emerges in relation to different types of dynamics on networks, in this work, we shall highlight that it is fundamentally a combinatorial one and is not a priori derived from any concrete dynamics running on the network. In other words, while we will consider that there is some kind of generic propagation—let it be information, electrons, or other types of particles hopping through the network—the theory presented hereafter does not require to specify which dynamical equations rule such propagation, as we focus on the structural (topological) constraints which generally affect such propagation. By analogy to the cases discussed in *SI Appendix*, S1.1 and S1.2 and (27), we call G_{ij} the structural propagator, which parsimoniously captures the role that the network's architecture plays in j receiving particles sent from i. Similarly, G_{ii} accounts for how much a node i structurally retains an item at it, as the

item returns to i infinitely often. For a particle initially located at the node i, the difference,

$$R_{i \to j}(\beta) = G_{ii}(\beta) - G_{ij}(\beta), \quad \textbf{[2]}$$

accounts for the opposition offered by the network structure to the directional displacement of a particle sent by node i to the node j, where the smaller the value of $R_{i \to j}$, the higher the probability that the particle does not get trapped at the origin i and can propagate to node j, i.e., there are more conductive walks between i and j than those returning back to the origin. In order to account for the resistance of the displacements between any pair of nodes, we should take into account the two possible directions of their mutual communication ($i \to j$ and $j \to i$). To this aim, one can symmetrize (2) to define the communication resistance between nodes i and j as $\xi_{ij}(\beta) := (R_{ij}(\beta) + R_{ji}(\beta))^{1/2}$. From the definition of the communicability function, and setting $\beta = 1$ without loss of generality, we obtain that the communication resistance reads:

$$\xi_{ij}^2 = \sum_{m=1}^n e^{\lambda_m} \left((\psi_m)_i - (\psi_m)_j \right)^2. \quad \textbf{[3]}$$

where $(\psi_m)_i$ is the i-th entry of the eigenvector associated with the m-th eigenvalue (λ_m) of $\mathbf{A}$. We rigorously proved that ξ_{ij} is an Euclidean distance (see *SI Appendix, section S2* for a proof). Conceptually, ξ_{ij} is a measure of the network resistance to a flow between i and j. Recently (43), it was proven that this communicability distance—and every spherical Euclidean distance—is the effective resistance between nodes in a network with given edge weights.

Network Geometrization and Resistive Shortest Paths. Since ξ_{ij} is an Euclidean distance and particles motion is confined to the network edges, we can proceed to the geometrization of the network (44, 45). To this aim, we first transform every edge of the graph into a compact 1-dimensional manifold. That is, for an edge $e = \{i, j\}$ we consider the boundary of the manifold to be $\partial e = i \cup j$. Then, each edge e inherits a metric g_e such that (e, g_e) is isometric to a finite interval $[0, L(e)]$ of the real line with the standard metric, where the length $L(e)$ is given by the communicability distance of the corresponding edge, i.e., $L(e) \equiv \xi_e = \xi_{ij}$. Finally, the distance metric on the edges is extended to the full graph via infima of lengths of curves in the geometrization of $\mathcal{G}$, such that the graph becomes a metrically complete length space (45).

Equipped with this geometrization, we can now define two different types of lengths for any given path $\mathfrak{p}(s \to t) = (s, \ldots, t)$ connecting nodes s and t in the network. First, the topological length $\ell_{\mathfrak{p}(s \to t)}$ of this path is just the number of edges in it. Among all paths $\{\mathfrak{p}(s \to t)\}$ connecting s and t, the one with the minimum length is denoted the shortest path $\mathrm{SP}(s, t)$ as

$$\mathrm{SP}(s, t) = \mathrm{argmin}_{\mathfrak{p}(s \to t)}[\ell_{\mathfrak{p}(s \to t)}]. \quad \textbf{[4]}$$

Observe that Eq. **4** can have more than one solution, specially for large networks *SI Appendix*, S4.

Second, and based on the geometrization induced by the communicability resistance above, we also define an effective length $\mathbb{L}_{\mathfrak{p}(s \to t)}$ by summing the induced length of each of the links involved in $\mathfrak{p}(s \to t)$:

$$\mathbb{L}_{\mathfrak{p}(s \to t)} = \sum_{(i,j) \in E \in \mathfrak{p}(s \to t)} \xi_{ij}. \quad \textbf{[5]}$$

[†] Yet sufficiently small so that the network is in the sparse regime.

At odds with $\ell_{\mathfrak{p}(s \to t)}$, which blindly assigns the same length (unity) to every edge of the network, $\mathbb{L}_{\mathfrak{p}(s \to t)}$ takes into account the topological neighborhoods of each of the nodes in the path and the associated likelihood that the particle might diffuse out of the path, accordingly. Likewise, it penalizes paths for which particles take naturally more time to travel due to the structure of the network in which the path is embedded. The specific path connecting s and t that minimizes this effective length is denoted the Shortest Resistive Path SRP(s, t), defined as:

$$\text{SRP}(s, t) = \text{argmin}_{\mathfrak{p}(s \to t)}[\mathbb{L}_{\mathfrak{p}(s \to t)}]. \qquad [6]$$

We are now ready to quantify i) the emergence of potential bypasses—i.e., the proliferation of non-SP between any two nodes—and ii) decide in a principled way when this path redundancy becomes relevant to the network function—something that, we advance, will happen when SRPs start to differ from SPs.

Communicability Entropy. To address the first question above, we now quantify, both microscopically and then at the network level, the degree by which, as disorder increases, new routes between edges become available. To this aim, let us return to the WS and BA models that we have considered before. As we have discussed, both the rewiring process and the BA mechanism create degree heterogeneities that intuitively make some a priori "inefficient" paths—e.g., long ones—to scale up in a predefined efficiency ranking (that would indeed be the case of path P_2 connecting nodes i and j in Fig. 1). Now, in practice, both WS and BA mechanisms can have heterogeneous effects on this reranking, depending on the particularities of the starting and ending nodes i and j (see *SI Appendix*, section S3 for an in-depth microscopic analysis on the effect of these local mechanisms on ξ_{ij} and $\mathbb{L}_{\mathfrak{p}(i \to j)}$). We first start by quantifying how these mechanisms generate a richness of possible trajectories connecting any pair of nodes i and j. The probability that a randomly intercepted trajectory indeed corresponds to one connecting i and j is

$$q_{ij} = \frac{G_{ij}}{\sum_{k<l} G_{kl}}. \qquad [7]$$

Then, the heterogeneity in the different number of choices for the trajectory of a particle, i.e., the trajectory richness of the network is given by the entropy

$$S(\mathbf{q}) = -\frac{1}{2} \sum_{i<j} q_{ij} \ln q_{ij}, \qquad [8]$$

that we call the communicability entropy. From an information-theoretic perspective, this entropy is a measure of the ignorance we have on who is the sender node and receiver node, when intercepting a message navigating the network. Since $0 \leq S(\mathbf{q}) \leq \ln(n(n-1)/2)$, the upper bound only reached when the set of probabilities $\mathbf{q}$ are uniform, we define a normalized version $\hat{S}(\mathbf{q}) := S(\mathbf{q})/\ln(n(n-1)/2)$.

Let us now analyze how $\hat{S}(\mathbf{q})$ behaves in our two reference frameworks. Intuitively, for a fixed mean degree $\langle k \rangle$, $\hat{S}(\mathbf{q})$ will increase in the WS model as p increases since rewiring increases trajectory richness. Likewise, in a BA model, one can vary the network's mean degree: For very small $\langle k \rangle$, the resulting BA network is almost tree-like, with no potential bypasses and thus low trajectory richness, whereas when we allow $\langle k \rangle$

to increase, additional routes are formed, thus increasing the trajectory richness; hence, $\hat{S}(\mathbf{q})$ should also increase. Fig. 2 *A* and *B* (red axis) confirm our intuitive arguments. In particular, in Fig. 2*A*, we observe that entropy grows rather quickly in a WS model for small rewiring probability $0 < p \leq 0.4$, reaching a steady maximum afterward. The impact of rewiring is notably stronger for small p, and this effect is emphasized further for SW networks of increasing $\langle k \rangle$. This behavior is easy to understand: In the small p region, there are few shortcuts, and each new one makes a difference. On the contrary, for large values of p, the entropy saturates very quickly to $\hat{S}(\mathbf{q}) \simeq 1$, i.e., the addition of more shortcuts does not make much of a difference beyond a certain p (see below for further analysis on the influence of the average degree). Fig. 2*B* reveals a similar behavior of $\hat{S}(\mathbf{q})$ for the BA model as the mean degree $\langle k \rangle$ increases (within the sparse regime for the BA preferential attachment mechanism to hold, see below), reaching full trajectory richness very quickly after a sudden increase in the region of small $\langle k \rangle$ values. In short, rewiring an ordered structure and increasing the link density of a heterogeneous network quickly (nonlinearly) boosts the trajectory richness and, thus, the amount of potential bypasses to any specific shortest path connecting any pair of nodes.

We now need to quantify when some of these new routes actually may become consolidated bypasses to shortest paths, like the situation illustrated in Fig. 1, where a particle traveling between two nodes i and j "might prefer" to use P_2, although being longer (in terms of number of edges to be traversed) than the shortest path P_1.

Bypass Consolidation and Associated Navigability Gain. To evaluate the impact of potential bypasses on the actual navigability, we use Eq. 5 and consider that, for any pair of nodes i and j, the SRP between i and j is a consolidated bypass to the shortest path(s) if the effective length of the SRP is smaller than the effective length of the (potentially many) SPs (i.e., $\mathbb{L}_{SRP}(i, j) < \mathbb{L}_{SP}(i, j)$ for all SPs connecting i and j). Interestingly, this criterion results to be equivalent to check that $\ell_{SRP(i,j)} > \ell_{SP(i,j)}$ (see *SI Appendix*, S4 for details). Once bypass detection is done, we need to quantify its impact. A measure that quantifies the impact of bypasses on the network's navigability is the topological length excess $\epsilon_{(i,j)}$

$$\epsilon_{(i,j)} = \left(1 - \frac{\ell_{\text{SP}(i,j)}}{\ell_{\text{SRP}(i,j)}} \right) \cdot 100, \qquad [9]$$

which indicates that, for a particle traveling between two arbitrary nodes i and j, choosing the consolidated bypass SRP over the SP, while beneficial according to the (hidden) network geometry, leads to an apparent excess of $\epsilon_{(i,j)}\%$ from the topological distance traveled via the shortest path. It turns out that Eq. 9 also quantifies the effective distance per link and the resulting gain of using SRP over SP (see *SI Appendix*, S4 for a full derivation of these metrics and their interpretation). To extract a global metric for the whole network, we just average $\epsilon_{(i,j)}$ over all pairs of nodes to define the network navigability gain:

$$\epsilon = \frac{2}{N(N-1)} \sum_{i<j}^{N} \epsilon_{(i,j)}. \qquad [10]$$

An illustration of these metrics in a toy network is given in *SI Appendix*, S5. Observe that ϵ quantifies an improvement of
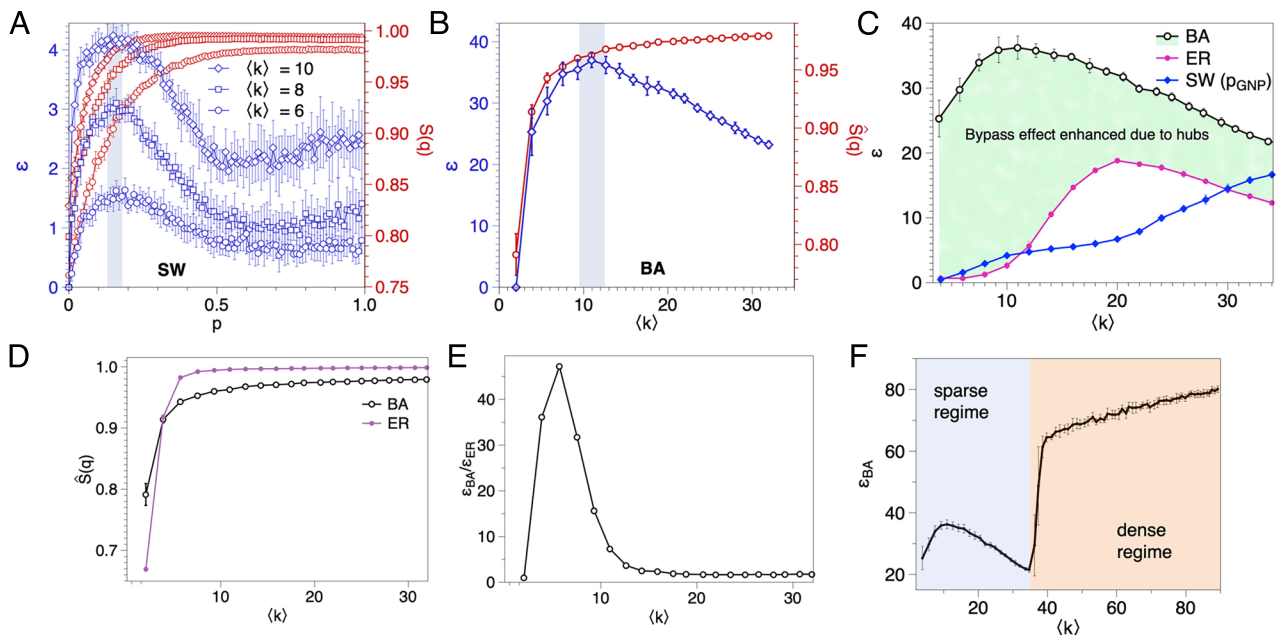
Fig. 2. Plot of the normalized communicability entropy $\hat{S}(\mathbf{q})$ (red) and of the net gain factor ϵ (blue) vs. : (A) the rewiring probability p for WS networks (numerical step of $\delta p = 0.01$) with $n = 250$ nodes and different average degree $\langle k \rangle$, or (B) the mean degree $\langle k \rangle$ of a BA model with $n = 250$ nodes. Each dot is the average of 100 realizations, and standard deviations over the ensemble of realizations are also depicted. In both panels, the shaded blue area highlights the maximum of ϵ and marks the network's good navigational point ($p_{\mathrm{GNP}} \approx 0.15$ for WS model, $\langle k \rangle_{\mathrm{GNP}} \approx 11$ for BA model). (C) ϵ vs $\langle k \rangle$ for networks of $n = 250$ nodes generated via the BA model, the WS model (poised at the good navigational point), and an Erdos-Renyi (ER) model for comparison. The bypass-induced navigability gain is substantially larger in heterogeneous (BA) networks than in more homogeneous ones. The comparison between ER and SW networks is nontrivial and can be explained in terms of the shapes of the respective degree distributions as $\langle k \rangle$ increases (see the text and *SI Appendix*). (D) Normalized communicability entropy of both BA and ER networks with the same number of nodes, as a function of the mean degree. (E) Ratio $\epsilon_{\mathrm{BA}}/\epsilon_{\mathrm{ER}}$ to highlight the difference in navigability gains displayed in panel (C). (F) ϵ_{BA} vs $\langle k \rangle$ in the extended region of high density, where preferential attachment is not properly working anymore (*SI Appendix*, S9), leading to an explosion of the navigability gain due to the transition to ultrashort graphs.

a function (network navigability) as a result of an innovation (consolidation of bypasses) and is therefore a quantitative proxy of structural deepening.

We can now quantify bypass consolidation and its associated navigability gain on relation to both WS and BA mechanisms. When we apply this formalism to the evolving SW network we obtain the results illustrated in Fig. 2 *A, Left* axis. We observe that the navigability gain factor ϵ exhibits a clear nonmonotonic shape as a function of the rewiring probability p. In fact, our measure detects a maximum for $p \approx 0.15$ at which, on average, traveling through the SRP is much more favorable than doing so through the SP. We call this probability the "good navigational point" (GNP) of the network, p_{GNP}. It is interesting to observe that p_{GNP} is a precise location inside the so-called small-world regime, which is independent of the network mean degree $\langle k \rangle$. Anecdotally, this value appears close to the saturating point of spectral spacing in SW networks (46, 47).

Now, note that the SW mechanism consolidates bypasses out of a regular-to-random transition, so comparatively speaking the values of ϵ should be typically higher in more structured networks—e.g., in networks with fat-tailed degree distributions like the BA model—where the presence of hubs makes the existence of bypasses even more necessary. This hypothesis is confirmed in Fig. 2 *B, Right* axis, in which ϵ reaches roughly values one order of magnitude larger in the BA model than those found in a comparable WS model. In this case, we observe again nonmonotonic behavior of ϵ with $\langle k \rangle$, displaying a maximum close to $\langle k \rangle \approx 11$, i.e., the BA model also has a good navigational point when mean degree is $\langle k \rangle_{\mathrm{GNP}} \approx 11$, where bypassing shortest paths that include hubs is maximally relevant.

To further analyze the impact of bypasses, we now compare the values of ϵ obtained in a BA model ($n = 250$ nodes and mean

degree $\langle k \rangle$) against i) those obtained for an Erdös-Renyi (ER) graph with the same n and $\langle k \rangle$—this latter being a model with the same number of edges but with a homogeneous (Poisson) degree distribution and thus virtually lacking any hubs—and ii) those of a WS model with the same n and same $\langle k \rangle$, and poised at $p = p_{\mathrm{GNP}}$. Results are shown in Fig. 2C and certify that, in the sparse regime ($\langle k \rangle < 35$), ϵ is substantially larger in BA than both ER and SW, i.e., the gain supported by bypasses is considerably more important in heterogeneous networks, as expected (48). When comparing the behavior of ϵ in ER vs SW networks (both in principle lacking substantial hubs), we observe an interesting effect: For a range of small mean degrees $\langle k \rangle < 11$, SW networks benefit more from bypasses than ER ones. The opposite is true for an intermediate $11 < \langle k \rangle < 30$, and the effect is again changed for very large mean degrees $\langle k \rangle > 30$. This nontrivial behavior can be explained by comparing the degree distributions of both ER networks and SW networks at p_{GNP} and by realizing the (often overlooked) fact that the degree distribution (in particular, the skewness and kurtosis) of an SW network poised at a fixed p undergoes different shapes as $\langle k \rangle$ increases (see *SI Appendix, section S8* for details). Incidentally, this can also explain why $\hat{S}(\mathbf{q})$ initial increase in SW networks is sharper for larger $\langle k \rangle$ (*SI Appendix*).

In summary, the effect of bypasses is maximized for SW networks at the good navigational point $p_{\mathrm{GNP}} \approx 0.15$, and within that point, this effect appears to be monotonically boosted when these SW networks increase their degree heterogeneity, i.e., increasing $\langle k \rangle$. ER networks have bypassing properties as long as they show degree heterogeneities, and to a small extent (Poisson distribution), this is the case. Such effect is then maximal around $\langle k \rangle \approx 20$ (the fact that bypasses have a nonmonotonic effect also within ER networks can again be explained in terms of the
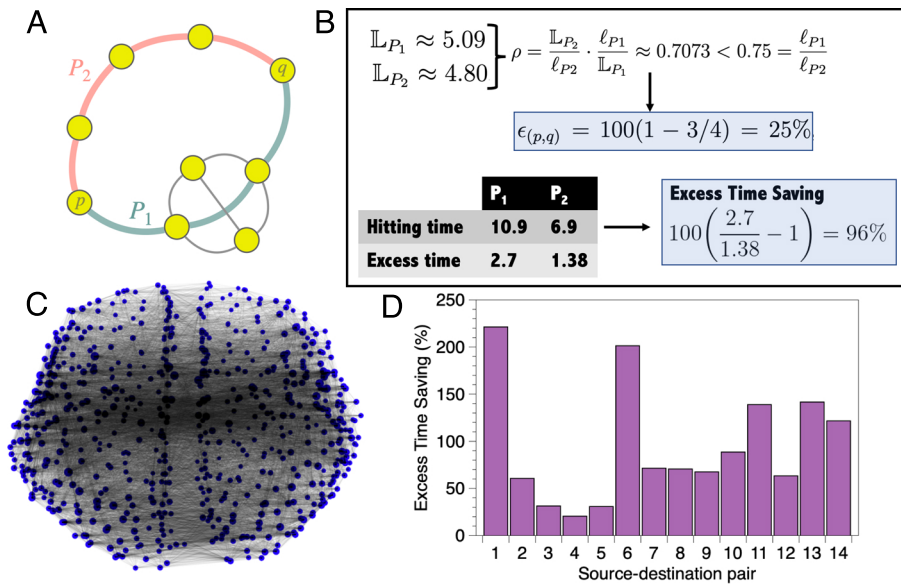
Fig. 3. (*A*) Toy network with a concrete source–destination pair (p, q), which can be navigated via paths P_1 and P_2. (*B*) Computation of the different metrics certifies that P_2 is a bypass of the shortest path P_1, and the navigability gain associated with this pair is 25% (a lower bound of the actual gain; see *SI Appendix*, S5). Random walk trajectories starting at p and eventually hitting q can be classified as P_1-like or P_2-like, depending on their specific trajectories (*SI Appendix*, S6). The hitting time and excess time of the P_1 class is larger than for P_2, meaning that random-walk navigability is enhanced in the P_2 (that is, the SRP) class. The excess time saving is a diffusion-proxy of the navigability gain (*SI Appendix*, S6). (*C*) Coactivation brain network. (*D*) Excess time saving for several source–destination pairs in the brain network, finding that SRP enhances navigability in all cases.

skewness degree distribution; see *SI Appendix*). Finally, in BA networks, bypassing effects are substantially larger due to higher degree heterogeneities, as expected.

To close this analysis, one can ask about the theoretical upper bound on ϵ. Heuristically, the effect of bypasses would be fully maximized in a situation where we add to a given (connected) network a new node that is linked to every other node. Such a new node would be a "superhub" that makes the network have shortest paths of length ≤ 2 for all pairs of nodes. In this extreme situation, many of the shortest paths will be systematically bypassed and ϵ would explode (see *SI Appendix, S9* for details). Now, is this just a theoretical scenario? It turns out that this situation can take place in an extreme version of the BA model in a finite graph, where $\langle k \rangle$ is large enough (compared to the initial seed) so that new nodes entering systematically connect to a large portion of the network, leading to so-called ultrashort graphs (49). This explosion is reported in Fig. 2*F*. Evidently, in this case, there is no preferential attachment anymore, so in some sense, the rationale behind the BA model breaks down in this dense regime[‡].

Effect on Dynamics. As already anticipated, our theory is purely structural and therefore dynamically agnostic and speaks of the effect of network geometrization on the formation of shortest paths in the geometrized network—the SRPs—which are different from the shortest paths of the original, ungeometrized network. Our contention is that these emergent bypasses have an effect on the network's navigability, and here, we provide an initial validation of this hypothesis by considering source–destination random walk trajectories navigating a network. Each of these random walk trajectories is then classified as SRP-like or SP-like depending on the specific sequence of nodes the walker is visiting (see *SI Appendix, S6* for details). One can subsequently compare the SRP class and the SP class by computing a number of quantities, such as the average hitting time in each class, or the

excess time (i.e., for each class, how much more time than the time spent by a ballistic walker it takes to reach the destination), which yield dynamical proxies for the effective length or the associated navigability gain defined above (*SI Appendix, S6*). Results for both a synthetic small network and for a large real network (a coactivation brain network, see below) are shown in Fig. 3 and confirm our hypothesis that particles are more prone to "get lost" (and thus spend a significantly longer time) navigating through a SP-like path compared to an SRP-like one. In other words, the presence of SRPs enhances navigability for diffusion-like dynamics (additional details and analysis are provided in *SI Appendix, S6*). At the same time, this finding further confirms that bypasses induce structural deepening by increasing the efficiency of network navigability.

We have also made some preliminary progress on analyzing how bypasses impact other network functions by considering two additional dynamical processes running on a network: synchronization and epidemic spreading. Results (fully detailed in *SI Appendix, section S7*) suggest that the prototypical dynamical fingerprints in each case (i.e., eigenratio of the Laplacian matrix for synchronization and epidemic threshold for epidemic spreading) are affected by bypass consolidation, and, in particular, qualitative dynamical changes occur in both types of dynamics close to p_{GNP}.

Empirical Networks. To round off, we have considered a total of 177 empirical networks of different nature, including social (4 collaboration networks of different nature, 3 termite mounds), biological (Human brain—70 anatomical, 70 functional at resting-state, one functional at task-driven (extracted and averaged from a meta-analysis of 1,600 works)—, neural network of *C. elegans*, a protein–protein interaction, a transcription yeast, 15 food webs), and technological ones (air transportation, Internet, 3 electronic circuits, power grid, 5 software networks), see *SI Appendix, section S11.1* for details and full references. Results on several metrics are summarized in Table 1, and some scatter plots are visualized in Fig. 4.

[‡]In the dense regime $\langle k \rangle > 35$, the calculations of ϵ need to be taken with caution as numerical rounding effects might become important when computing exp (*A*).

Table 1. Summary of metrics for empirical networks, depicting the communicability entropy $\hat{S}(q)$, the navigability gain ϵ, the optimal rewiring probability p^*, and the navigability ratio ϵ/ϵ_{BA} (see the text) across 177 different empirical networks (for many of them, we offer averages; see *SI Appendix*, S10 for details), where: Human brain (anatomical) provides the averaged results across 70 anatomical networks (using the same parcellation), Human brain (functional, resting-state) provides the averaged results across 70 functional networks (using the same parcellation as the anatomical networks), Software provides the averaged results across the networks MySQL, XMMS, Abi, Digital, and VTK; Food webs is the average of 15 food webs (see *SI Appendix*, S11.3 for disaggregation); Electronic circuits is the average of three electronic circuits; Termite mounds is the average of three termite mounds

Network	$\hat{S}(q)$	ϵ (%)	p^*	ϵ/ϵ_{BA}
Human brain (functional, task-driven)	0.9234	51.71	0.30	0.78
Collaboration CoGe	0.7776	41.50	0.21	0.93
Collaboration QcGr	0.4598	38.39	0.15	0.79
Human brain (anatomical)	0.925 ± 0.022	36.21 ± 1.52	0.23 ± 0.01	0.86 ± 0.04
C. elegans neurons	0.9312	31.69	0.34	0.87
USA airports 1997	0.8501	28.60	0.27	0.76
Internet AS 1997	0.8891	25.49	~ 1	0.52
Yeast PPI	0.8344	25.50	0.24	0.55
Drugs users	0.7794	21.18	0.10	0.57
Software	0.8308 ± 0.0263	21.11 ± 12.10	$\sim 1^\dagger$	0.58
Human brain (functional, resting-state)	0.758 ± 0.054	20.81 ± 1.42	0.17 ± 0.02	0.49 ± 0.05
Roget thesaurus	0.9215	19.18	0.35	0.43
Transcription yeast	0.8128	12.26	~ 1	0.38
Food webs	0.9498 ± 0.0208	9.94 ± 7.13	**	0.64***
electronic circuits	0.8202 ± 0.0260	3.456 ± 2.561	~ 1	0.12
Termite mounds	0.5707 ± 0.0331	3.100 ± 2.12	~ 1	0.11
Power grid	0.6348	2.61	~ 1	0.05

†Except MySQL which has $p^* \approx 0.29$. **Three types of behaviors: i) $p^* \approx 1$ for 8 food webs; ii) $0.43 \leq p^* \leq 0.45$ for El Verde, Shelf, Ythan1, and Ythan2; iii) $0.03 \leq p^* \leq 0.14$ for Bridge Brooks, Coachella, and Little Rock. *** See *SI Appendix*, section S11 for disaggregated data and additional details.

The first two columns of this table report the normalized communicability entropy $\hat{S}(q)$ and navigability gain ϵ. Interestingly, all of them appear to be entropic enough for potential bypasses to have been formed, as values of $\hat{S}(q)$ are in the region where our analysis on synthetic models show consolidated bypasses§. We indeed find that essentially all real-world networks harbor consolidated bypasses ($\epsilon > 0$), albeit with different impacts, what allows us to rank them accordingly. At the top of the ranking, the net gain induced by consolidated bypasses reaches over 50% for the (task-driven) functional brain network, followed by many other self-organized networks (collaboration networks, *C. elegans*, etc). It is interesting to see that the navigability gain substantially drops for functional brain networks when passing from task-driven activation to resting state. This might be suggesting the possibility that navigability gain in functional brain networks might be task-related, something that deserves further research. Our finding that the navigability gain of anatomic networks is in between those of task-driven and resting-state functional networks is reasonable. On one hand, resting-state function in adults is usually thought to be restricted to a brain module. On the other hand, the specific task-driven network that we analyze here is the outcome of a meta-analysis of over 1,600 works considering different tasks—and thus, in principle, the result of multiple brain modules. These hypotheses await confirmation and, in any case, further research is needed to elucidate the relation of the topology-induced bypasses studied here with specific cognitive aspects.

At the bottom of the list in Table 1, we find some designed networks, such as electronic circuits or the power grid, the latter having only a discrete 2.6% navigability gain. This can be indicative that the power grid, while having hubs to some extent (4, 50), has not evolved according to mechanisms such as WS or BA, is not self-organized, and, as a consequence, does not hold the necessary preemptive structural bypasses to avoid systemic failures, as we have seen during blackouts (51). Note at this point that the navigability gain ϵ does not trivially correlate with more standard network metrics, such as network density (linear regression of the scatter plot offers a $R^2 = 0.12$), mean degree ($R^2 = 0.09$), average path length ($R^2 = 0.01$), or average clustering ($R^2 = 0.006$), see *SI Appendix*, S11.4 for details.

Now, to which extent the observed bypasses are indeed of the SW-type (i.e., bypassing shortest paths consistently generated via a WS-like mechanism), and in such case, how close empirical networks are to their theoretical good navigational point? While this question is difficult to answer, the metric p^* reported in the third column of Table 1 (Fig. 4) provides a first step. Operationally, for a given empirical network $\mathcal{G}$ with n nodes and mean degree $\langle k \rangle$, we estimate the closest purely SW-generated network $\mathcal{G}'(p)$ (with the same $(n, \langle k \rangle)$). This is achieved by minimizing the spectral dissimilarity distance $\mathcal{D}(\mathcal{G}, \mathcal{G}') = \sqrt{\sum_{j=1}^{n} \left(\lambda_j(\mathcal{G}) - \lambda_j(\mathcal{G}') \right)^2}$, where $\lambda_j(\mathcal{G})$ is the j-th eigenvalue of the adjacency matrix of network $\mathcal{G}$ and minimization is over p, i.e., $p^* = \text{argmin}_p[\mathcal{D}(\mathcal{G}, \mathcal{G}'(p)]$¶. This metric indicates that networks can be typically clustered in two types: one (which includes all human brain networks, the neural

§Note, however, that a finer analysis is needed as, e.g., we have observed in the SW analysis that reaching the GNP is density-dependent, i.e., the communicability entropy saturates quicker as p increases for networks with larger mean degree.

¶Note that this analysis is not designed to find which real-world networks can be classified as small-world. It just assumes they all have such ingredient in their network formation and evaluate, setting that prior as the sole generating mechanism, what would then be the value of the rewiring probability, so as to establish whether the bypass amount is close or not to the GNP. For those networks whose p^* is found to be close to the GNP, this is partial evidence that such network harbors bypasses of the SW-type.
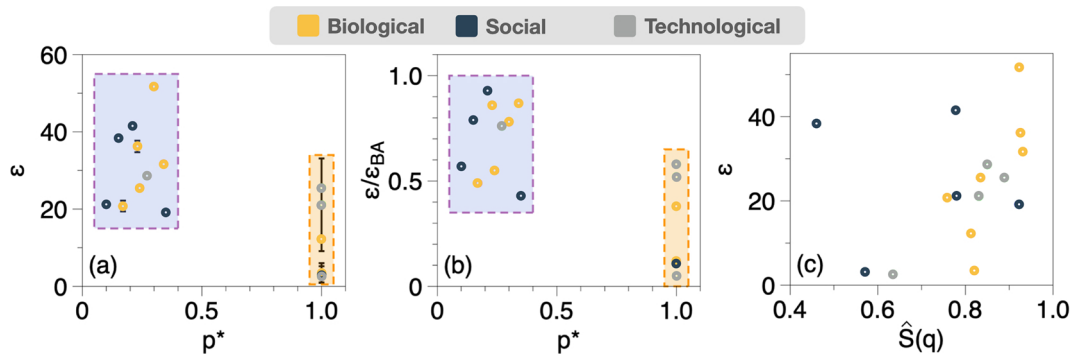
Fig. 4. Some scatter plots of the metrics reported in Table 1 for empirical networks. (*Left*) Net navigability gain ϵ vs p^*, revealing the emergence of two well-defined groups of networks. (*Centre*) Navigability ratio ϵ/ϵ_{BA} vs. p^*, finding the same clustering as in panel (*left*). (*Right*) ϵ vs. the normalized communicability entropy $\hat{S}(\mathbf{q})$, where no clear clustering emerges .

network of *C.elegans*, the protein–protein interaction network, collaboration networks, Roget network, and the US air network) where $\mathcal{D}(\mathcal{G}, \mathcal{G}'(p))$ has a nonmonotonic shape with a minimum $p^* \in [0.15, 0.35]$—i.e., close but not exactly at the good navigational point—and another cluster of networks (including electronic circuits, Internet AS97, software networks of termite mounds) where $\mathcal{D}(\mathcal{G}, \mathcal{G}'(p))$ is monotonically decreasing and thus $p^* = 1$ (see *SI Appendix*, S11.2 for further details and analysis). The former class thus tends to harbor bypasses of the SW-type—avoiding shortcuts—and its network formation includes at least partially some SW ingredient while the second one tends to have a structure which cannot be well explained only by SW mechanisms (this does not mean, however, that such network is random). Incidentally, no clear function-related clustering emerges.

The fourth column of Table 1 finally depicts ϵ/ϵ_{BA}—where ϵ_{BA} is the navigability gain of a BA network with the same number of nodes n and mean degree $\langle k \rangle$ of the real network—and quantifies whether the observed network bypasses are effectively bypassing hubs. This metric highlights two different groups of networks. The first group is characterized by the relevance of hubs (i.e., $\epsilon/\epsilon_{BA} \sim 1$). In the second group of networks the hubs are not necessarily playing a fundamental role in terms of the consolidated bypasses. That is, either the bypasses are not necessarily skipping hubs, or such networks have not been designed to harbor bypasses. In closing, they do not abide to a BA-like mechanism, so ϵ/ϵ_{BA} is closer to zero (see *SI Appendix,* S11.3 for further discussion).

Discussion

The journey of network complexification is supported by basic mechanisms including the celebrated WS and BA, among others. As the network evolves accordingly, we have shown that it naturally increases its communicability entropy $S(\mathbf{q})$ and, in so doing, it allows for new navigational routes to be built, entropically providing bypass "candidates" to the network. Our theory allows to detect when some of these new routes consolidate their bypassing property by subsequently getting to be more favorable than the corresponding shortest paths connecting the same pairs of nodes, and we show that consolidation takes place in both WS and BA models. Interestingly, we find that the role of bypasses is maximized in a small parameter region—which we call the network's good navigational point—located in a point inside the Small-World regime and for a specific mean degree in the BA model. These findings suggest that the navigation gain offered by the network bypasses is

indeed reflecting a form of structural deepening, thus putting the onset of complexity in networks into a solid quantitative footing.

We have certified that bypasses induce clear navigation gain for particles undergoing diffusion-like dynamics and also play an effect on other network functions, including harboring synchronization and epidemic spreading. We have then shown that many empirical networks considered complex, including brain networks, indeed have good navigational point properties, while those that are not cataloged as self-organized but have been designed tend to not include bypasses in their design, with well-known unfortunate consequences (51).

In hindsight, our results could provide a theoretical and mechanistic support for the role of bypasses in, e.g., physiological systems—where plasticity is of utmost importance (52). First, network bypasses naturally relate to the existence of the so-called "collateral circulation": a system of specialized endogenous bypass vessels present in most tissues providing protection against ischemic injury caused by ischemic stroke, coronary atherosclerosis, peripheral artery disease, and other conditions and diseases (53). Second, in brain networks, there is nowadays enough observational evidence which supports that these are SW in the Watts–Strogatz sense (54) and possess hubs which create skewness of their degree distributions (55). At the same time, recent experiments (56) suggest that propagating signals in the brain using hubs as part of the navigation path might have a large energetic cost, triggering research on nongeodesic information propagation (56–58). Our work indeed supports the concept of nongeodesic navigability (via network bypasses) and reconciles this with the reported network structure. In this context, note that (59) proposed considering networks of neurons as evolving and growing connections in a distributed fashion (via mechanisms different that SW or BA) such that shortest path minimization and robustness maximization (which in general implied to avoid the creation of hubs) was performed at the same time. Note, however, that brain navigation is not likely to occur always geodesically (56–58) (this also would imply that individual neurons perform global optimization and have access to the whole brain structure). The logical conclusion is that the seminal findings in ref. 59 imply that the creation of shortest paths should be accompanied by the proliferation of additional structure that plays a role of structural deepening, in good agreement with our theory.

Third, in another recent work (60), it has been shown that brain function appears to be robust against damage by readapting and repurposing nondamaged links, something that can be interpreted to the brain's ability to recompute SRPs and thus

rerank bypasses after network damage. All in all, elucidating the impact of our findings in the context of neuroscience is an exciting avenue for future work.

An aspect not explored in this paper but also of major interest is the implications of our theory to congestion or jamming phenomena in networks and to which extent our proposed measures of topological length excess and navigability gain could anticipate congestion in, e.g., transportation and urban systems. First, we should disclose that conceptually similar problems have been theorized in the mathematics literature, where some authors have studied the so-called "resistance distance" in networks (61)—where some unit resistances are placed at every edge in a network—in the context of congestion (62, 63). Now, while an interesting mathematical concept, this latter distance analytically converges, for large graphs and in high dimensions, to an expression that does not take into account the structure of the graph (64) (i.e., it only depends on the degrees of the source and destination nodes) and thus unfortunately turns useless in real-world scenarios#. Second, recent empirical evidence in urban science indeed suggests that, at rush hours, in different cities worldwide, paths which can be identified as SRPs are supporting more traffic than SPs (65), i.e., they become systematically preferred routes. This constitutes preliminary support in favor of the relevance of SRPs for navigation strategies in networks subject to jamming, and further research is deserved. For instance, we speculate that this strategy can be further refined by, instead of systematically selecting only the SRP as the preferred route, ranking each of the paths connecting any two locations via the computation of its associated topological length excess and rerouting traffic accordingly when needed.

#Anecdotally, it is easy to see that such resistance distance is already unable to capture the nuanced navigability properties of paths P1 and P2 in the toy network presented in Fig. 3 (revealed by the hitting times analysis) and that in turn our theory correctly predicts.

Other important open questions for further research include understanding the role played by network bypasses and their relation to structural deepening in other mechanistic growth models (e.g., assortative/disassortative mixing, triadic closure, etc), and the extension of our theory to weighted (see a preliminary discussion on this topic in *SI Appendix*, S10), temporal and higher-order networks (66, 67).

Finally, while network bypass emergence appears to be contingent on the growth mechanism—and thus appears to be a by-product of it—bypass consolidation (structural deepening) is the effect which probably makes those growth mechanisms to be sustainable in the first place. Simply put, we argue, bypasses sustain complexity.

1. E. Estrada, *The Structure of Complex Networks: Theory and Applications* (Oxford University Press, Oxford, UK, 2012).
2. V. Latora, V. Nicosia, G. Russo, *Complex Networks: Principles, Methods and Applications* (Cambridge University Press, Cambridge, UK, 2017).
3. D. J. Watts, S. H. Strogatz, Collective dynamics of "small-world" networks. *Nature* **393** (1998), 440–442 (1998).
4. A. L. Barabasi, R. Albert, Emergence of scaling in random networks. *Science* **286**, 509–512 (1999).
5. J. Tranquillo, *An Introduction to Complex Systems: Making Sense of a Changing World* (Springer-Nature, Switzerland, 2019), pp. 314–315.
6. W. B. Arthur, *Increasing Returns and Path Dependence in Economy* (University of Michigan Press, Ann Arbor, USA, 1994).
7. A. D. Broido, A. Clauset, Scale-free networks are rare. *Nat. Commun.* **10**, 1–10 (2019).
8. P. Holme, Rare and everywhere: Perspectives on scale-free networks. *Nat. Commun.* **10**, 1–3 (2019).
9. X. Xiao, H. Chen, P. Bogdan, Deciphering the generating rules and functionalities of complex networks. *Sci. Rep.* **11**, 22964 (2021).
10. Y. Xue, P. Bogdan, Reliable multi-fractal characterization of weighted complex networks: Algorithms and implications. *Sci. Rep.* **7**, 7487 (2017).
11. R. Albert, H. Jeong, A. L. Barabasi, Error and attack tolerance of complex networks. *Nature* **406**, 378–382 (2000).
12. E. Berthier, M. A. Porter, K. E. Daniels, Forecasting failure locations in 2-dimensional disordered lattices. *Proc. Natl. Acad. Sci. U.S.A.* **116**, 6742–16749 (2019).
13. P. Echenique, J. Gómez-Gardeñes, Y. Moreno, Dynamics of jamming transitions in complex networks. *EPL (Europhys.)* **Lett.) 71**, 325 (2005).
14. L. Lacasa, M. Cea, M. Zanin, Jamming transition in air transportation networks. *Phys. A* **388**, 3948–3954 (2009).
15. J. Duch, A. Arenas, Scaling of fluctuations in traffic on complex networks. *Phys. Rev. Lett.* **96**, 218702 (2006).
16. L. Zhao, Y. C. Lai, K. Park, N. Ye, Onset of traffic congestion in complex networks. *Phys. Rev. E* **71**, 026125 (2005).
17. J. Goñi *et al.*, Exploring the morphospace of communication efficiency in complex networks. *PLoS One* **8**, e58070 (2013).
18. J. Gómez-Gardeñes, V. Latora, Entropy rate of diffusion processes in complex networks. *Phys. Rev. E* **78**, 065102 (2008).
19. K. Sneppen, A. Trusina, M. Rosvall, Hide-and-seek on complex networks. *EPL (Europhys.)* **Lett.) 69**, 853 (2005).
20. M. Rosvall, A. Gronlund, P. Minnhagen, K. Sneppen, Searchability of networks. *Phys. Rev. E* **72**, 046117 (2005).
21. O. Sporns, *Networks of the Brain* (MIT Press, Cambridge, USA, 2011).
22. J. Goñi *et al.*, Resting-brain functional connectivity predicted by analytic measures of network communication. *Proc. Natl. Acad. Sci. U.S.A.* **111**, 833–838 (2013).
23. E. Estrada, Informational cost and networks navigability. *Appl. Math. Comput.* **397**, 125914 (2021).
24. U. Von Luxburg, A. Radl, M. Hein, Getting lost in space: Large sample analysis of the commute distance. *Adv. Neural Inf. Process. Syst.* **23**, 2622–2630 (2010).
25. R. K. Ahuja, T. L. Magnanti, J. B. Orlin, *Network Flows* (MIT, 1988).
26. E. Estrada, N. Hatano, Communicability in complex networks. *Phys. Rev. E* **77**, 036111 (2008).
27. E. Estrada, N. Hatano, M. Benzi, The physics of communicability in complex networks. *Phys. Rep.* **514**, 89–119 (2012).
28. E. Estrada, N. Hatano, Statistical-mechanical approach to subgraph centrality in complex networks. *Chem. Phys. Lett.* **439**, 247–251 (2007).
29. C. H. Lee, S. Tenneti, D. Y. Eun, "Transient dynamics of epidemic spreading and its mitigation on large networks" in *Proceedings of the Twentieth ACM International Symposium on Mobile Ad Hoc Networking and Computing* (2019), pp. 191–200.
30. P. Bartesaghi, E. Estrada, Where to cut to delay a pandemic with minimum disruption? Mathematical analysis based on the SIS model *Math. Models Methods Appl.* **31**, 2571–2596 (2021).
31. L. A. Fernandez, "Synchronization in complex networks under uncertainty," Doctoral dissertation, Universitat Rovira i Virgili, Chapter 6 (2022).
32. F. Zamani Esfahlani, J. Faskowitz, J. Slack, B. Misic, R. F. Betzel, Local structure-function relationships in human brain networks across the lifespan. *Nat. Commun.* **13**, 1–16 (2022).
33. A. Arnatkeviciute *et al.*, Genetic influences on hub connectivity of the human connectome. *Nat. Commun.* **12**, 1–14 (2021).
34. Jonathan J. Crofts, Desmond J. Higham, A weighted communicability measure applied to complex brain networks. *J. R. Soc. Interface* **6**, 411–414 (2009).
35. J. J. Crofts *et al.*, Network analysis detects changes in the contralesional hemisphere following stroke. *Neuroimage* **54**, 161–169 (2011).
36. I. M. Campbell, R. A. James, E. S. Chen, C. A. Shaw, NetComm: A network analysis tool based on communicability. *Bioinformatics* **30**, 23 (2014).
37. E. Lella *et al.*, Communicability disruption in Alzheimer's disease connectivity networks. *J. Complex Netw.* **7**, 83–100 (2019).
38. R. F. Betzel, S. Gu, J. D. Medaglia, F. Pasqualetti, D. S. Bassett, Optimally controlling the human connectome: The role of network topology. *Sci. Rep.* **6**, 1–14 (2016).
39. C. Seguin, O. Sporns, A. Zalesky, F. Calamante, Network communication models narrow the gap between the modular organization of structural and functional brain networks. *NeuroImage* **119323** (2022).
40. J. Serra-Musach *et al.*, Cancer network activity associated with therapeutic response and synergism. *Genome Med.* **8**, 1–12 (2016).

41. L. Mander *et al.*, A morphometric analysis of vegetation patterns in dryland ecosystems. *R. Soc. Open Sci.* **4**, 160443 (2017).
42. Y. Li, C. W. Zobel, O. Seref, D. Chatfield, Network characteristics and supply chain resilience under conditions of risk propagation. *Int. J. Prod. Econ.* **223**, 107529 (2020).
43. E. Estrada, Every nonsingular spherical Euclidean distance matrix is a resistance distance matrix. *Linear Algebra Appl.* **656**, 198–209 (2023).
44. S. Markvorsen, Minimal webs in Riemannian manifolds. *Geom. Dedicata* **133**, 7–34 (2008).
45. M. R. Bridson, A. Haefliger, *Metric Spaces of Non-Positive Curvature* (Springer Science & Business Media, 2013), vol. 319.
46. H. Yang, F. Zhao, B. Wang, Synchronizabilities of networks: A new index. *Chaos* **16**, 043112 (2006).
47. G. Zhu, H. Yang, C. Yin, B. Li, Localizations on complex networks. *Phys. Rev. E* **77**, 066113 (2008).
48. C. I. Del Genio, T. Gross, K. E. Bassler, All scale-free networks are sparse. *Phys. Rev. Lett.* **107**, 17 (2011).
49. G. Zamora-López, R. Brasselet, Sizing complex networks. *Comms. Phys.* **2**, 144 (2019).
50. B. Hartmann, V. Sugar, Searching for small-world and scale-free behaviour in long-term historical data of a real-world power grid. *Sci. Rep.* **11**, 1–10 (2021).
51. S. Mei, X. Zhang, M. Cao, *Power Grid Complexity* (Springer Science & Business Media, 2011).
52. M. Gosak, M. Milojević, M. Duh, K. Skok, M. Perc, Networks behind the morphology and structural design of living systems. *Phys. Life Rev.* **41**, 1–21 (2022).
53. J. E. Faber, W. M. Chilian, E. Deindl, N. van Royen, M. A. Simons, Brief etymology of the collateral circulation. *Arterioscler. Thromb. Vasc. Biol.* **34**, 1854–1859 (2014).
54. D. S. Bassett, E. D. Bullmore, Small-world brain networks. *Neuroscientist* **12**, 512–523 (2006).
55. M. P. Van den Heuvel, O. Sporns, Network hubs in the human brain. *Trends Cogn. Sci.* **17**, 683–696 (2013).
56. T. Dardo, G.-J. Wang, N. D. Volkow, Energetic cost of brain functional connectivity. *Proc. Natl. Acad. Sci. U.S.A.* **110**, 13642–13647 (2013).
57. S. Caio, M. P. Van Den Heuvel, A. Zalesky, Navigation of brain networks. *Proc. Natl. Acad. Sci. U.S.A.* **115**, 6297–6302 (2018).
58. A. Avena-Koenigsberger, B. Misic, O. Sporns, Communication dynamics in complex brain networks. *Nat. Rev. Neurosci.* **19**, 17–33 (2018).
59. C. Yin et al., Network science characteristics of brain-derived neuronal cultures deciphered from quantitative phase imaging data. *Sci. Rep.* **10**, 15078 (2020).
60. G. Rapisardi, I. Kryven, A. Arenas, Percolation in networks with local homeostatic plasticity. *Nat. Commun.* **13**, 1–9 (2022).
61. D. Klein, M. Randic, Resistance distance. *J. Math. Chem.* **12**, 81–95 (1993).
62. E. Grippo, E. A. Jonckheere, Effective resistance criterion for negative curvature: Application to congestion control. *IEEE Conf. Control Appl.*, 129–136 (2016).
63. E. Jonckheere, E. Grippo, R. Banirazi, Curvature, entropy, congestion management and the power grid. *IEEE Conf. Control Technol. Appl*, 535–542 (2019).
64. U. Von Luxburg, A. Radl, M. Hein, Getting lost in space: Large sample analysis of the commute distance. *Adv. Neural Inf. Process Syst.* **23**, 2622–2630 (2010).
65. M. Akbarzadeh, E. Estrada, Communicability geometry captures traffic flows in cities. *Nat. Hum. Behav.* **2**, 645–652 (2018).
66. F. Battiston, F, G. Cencetti, I. Iacopini, V. Latora, M. Lucas, A. Patania, J.G. Young, and G. Petri., Networks beyond pairwise interactions: Structure and dynamics. *Phys. Rep.* **874**, 1–92 (2020).
67. S. Majhi, M. Perc, D. Ghosh, Dynamics on higher-order networks: A review. *J. R. Soc. Interface* **19**, 20220043 (2022).
68. E. Estrada, J. Gómez-Gardeñes, L. Lacasa, Codes. Github. https://github.com/lucaslacasa/bypasses. Deposited 8 July 2023.